Projectile- and charge-state-dependent electron yields from ion penetration of solids as a probe of preequilibrium stopping power

Hermann Rothard*
Institut für Kernphysik der Johann-Wolfgang-Goethe-Universität, August-Euler-Strasse 6, D-6000 Frankfurt am Main 90, Federal Republic of Germany

Jørgen Schou
Risø National Laboratory, Physics Department, DK-4000 Roskilde, Denmark

Karl-Ontjes Groeneveld
Institut für Kernphysik der Johann-Wolfgang-Goethe-Universität, August-Euler-Strasse 6, D-6000 Frankfurt am Main 90, Federal Republic of Germany

(Received 24 July 1991)

Kinetic electron-emission yields γ from swift ion penetration of solids are proportional to the (electronic) stopping power $\gamma \sim \beta S^*$, if the preequilibrium evolution of the charge and excitation states of the positively charged ions is taken into account. We show that the concept of the *preequilibrium near-surface stopping* S^* can be applied successfully to describe the dependence of the ion-induced electron yields on the projectile atomic number Z_P and on the charge states q_i of the incoming ions. We discuss the implementation of this concept into Schou's transport theory after having presented a summary of recent results on the projectile- and charge-state dependence of forward and backward electron yields γ_F and γ_B and the Meckbach factor $R=\gamma_F/\gamma_B$. A simple extension of the yield equations is proposed and several assumptions are justified by investigating the "transport factor" β, the energy spectrum of directly ejected recoil electrons and the evolution of ionic charge state inside solids. Estimates of the energy-loss fraction leading to electron emission and the effective charges of the ions near the surface allow a quantitative description of the Z_P dependence of the electron yields.

PACS number(s): 79.20.Rf, 34.90.+q

I. INTRODUCTION

The interaction of swift charged particles ($v_p > 1$ keV/u) with solids leads to the so-called "kinetic emission of electrons" [1]. This basic phenomenon is related to the (electronic) energy loss per unit path length, i.e., the stopping power S_e of the particles. Consequently, most of the theoretical approaches [1] consider the yield γ of electrons ejected per incident projectile to be proportional to the electronic stopping power, $\gamma \sim S_e$, or

$$\gamma = \Lambda S_e \ . \tag{1}$$

In order to study the validity of Eq. (1), it became common practice [1,2] to define parameters

$$\begin{aligned} \Lambda_B^* &= \gamma_B / S_e \quad \text{for the } \textit{backward} \text{ yield} , \\ \Lambda_F^* &= \gamma_F / S_e \quad \text{for the } \textit{forward} \text{ yield} , \\ \Lambda_T^* &= \gamma_T / S_e = \Lambda_B^* + \Lambda_F^* \quad \text{for the } \textit{total} \text{ yield} , \end{aligned} \tag{2}$$

as ratios of the measured electron yields γ and the (tabulated) stopping-power values S_e. Here, γ_F denotes the yield of electrons emitted in the forward hemisphere, i.e., the yield from the exit surface in the direction of the ions, γ_B is the backward-electron yield, and the total yield is $\gamma_T = \gamma_F + \gamma_B$.

The important assumption Eq. (1) has been confirmed experimentally for proton impact, i.e., the parameters Λ^* obtained from Eq. (2) were found to be constant within a wide projectile-energy range, 5 keV $\leq E_P \leq$ 24 MeV [1]. Furthermore, a rough overall proportionality of total electron yields from thin foils, $S_e \sim \gamma_T$ (within a factor of 2), has been observed for a variety of projectile nuclear charges Z_P ($1 \leq Z_P \leq 92$) in a wide range of projectile velocities v_P (15 keV/u $\leq E_P/M_p \leq$ 46 MeV/u) over four decades of stopping power and total electron-yield values [2]. The electron yields scale with the stopping power of the ions, even for relativistic heavy ions (Ar) at the heavy-ion synchrotron (GSI-SIS) of the Gesellschaft für Schwerionenforschung at Darmstadt (up to 1.65 GeV/u) [3].

In this context, experiments on electron emission from *thin solid foils* provide us with very detailed information, because a considerable proportion of the projectile-energy loss leads to the creation of high-energy electrons, which are predominantly ejected in the forward direction. In particular, the target-thickness dependence of electron emission is strongly related to the equilibration of the ionic charge states and thus yields unique information on the preequilibrium of charge-exchange and projectile-excitation processes [2,4–6].

Since the first investigation of electron emission from *thin foils* in 1931 [7], some papers have been published

concerning measurements of the total electron yield, $\gamma_T=\gamma_B+\gamma_F$ [8–10]. Other authors have studied the emission of electrons from the entrance and the exit surfaces of thin foils separately [2,5,11–18]. This allows us to study the "Meckbach factor," i.e., the ratio of the forward to the backward yield, $R=\gamma_F/\gamma_B$, which was introduced in 1975 by Meckbach, Braunstein, and Arista [11]. Although ion-induced electron emission strongly depends on surface properties [1,2,9,19,20], only two groups have been able to perform experiments with thin foils in ultrahigh vacuum under controlled surface conditions [1,2,9,17–20].

It is the aim of this paper to demonstrate that the proportionality of electron yields γ and stopping power S_e [Eq. (1)] holds—not only for proton-bombardment, but even for heavy-ion bombardment of solids if the preequilibrium evolution of the charge state of the ions is taken into account properly. The preequilibrium near-surface stopping power $S_e^*\sim q^{*2}$ is proportional to the square of the depth (x) dependent effective ion charge $q^*(x)$ and thus deviates from tabulated bulk energy-loss values. This concept can be used to describe the electron-yield dependence on the projectile atomic number Z_P as well as the dependence of electron yields on the charge state q_i of the incoming ions.

II. THEORY: EQUATIONS FOR HEAVY-ION-INDUCED ELECTRON YIELDS

Rothard *et al.* reported a dependence of the ratios Λ^* of electron yields to the (electronic) stopping power on the projectile atomic number (Z_P) of ions with incoming charge $q_i=1$ [2],

$$\Lambda^*(\mathrm{H})>\Lambda^*(\mathrm{He})>\Lambda^*(\mathrm{Ne}) . \tag{3}$$

The experiments were performed with sputter-cleaned foils of C, Al, Ti, Ni, and Cu at projectile energies around $E_p/M_p\approx 60-600$ keV/u, and the relation (3) was found to hold both for the backward yields γ_B and the forward yield γ_F. The energy-loss values were calculated following Ziegler, Biersack, and Littmark (ZBL) [21] to obtain the ratios $\Lambda_B^*=\gamma_B/S_{\mathrm{ZBL}}$ and $\Lambda_F^*=\gamma_F/S_{\mathrm{ZBL}}$ according to Eq. (2). At this point, it should be noted that we have used ZBL stopping-power tables throughout this paper, since these tabulations are the only existing ones for all possible beam-target combinations.

The results of Ref. [2] were discussed within a simple extension of Schou's transport theory for electron emission by charged particles [22] as caused by a deviation of the effective near-surface stopping power S^* in comparison to the ZBL values. S^* takes into account that the major part of the electrons originate from a depth within about 10 Å below the surface of the solid, where the effective charge of the ions, determining their energy loss, may significantly differ from the charge-equilibrium ZBL values.

As an important result of the transport theory [1,22], the electron yields per *proton* are given by

$$\begin{aligned}\gamma_B&=\Lambda^*\beta S ,\\ \gamma_F&=\Lambda^*(1-\beta)S .\end{aligned} \tag{4}$$

In the particular case of *proton* impact at sufficiently high velocities ($v_p>50-100$ keV/u) where

$$S_B^*(Z_P=1)=S_F^*(Z_P=1)=S_{\mathrm{ZBL}}(Z_P=1) \tag{5}$$

can be assumed, Eq. (1) is fulfilled strictly. Thus the parameters Λ^* obtained from Eq. (2) for *protons* can be regarded as the true "material parameters"

$$\Lambda(Z_T)=\Lambda_F^*/(1-\beta)=\Lambda_B^*/\beta=\Lambda_T^* \tag{6}$$

which depend on target properties (such as ionization cross sections, the low-energy electron stopping power, transport lengths, and the height of the surface potential barrier) only. Such material parameters $\Lambda(Z_T)$ from proton bombardment of thin foils have been measured by Clouvas *et al.* [9] and Rothard *et al.* [17] for 11 different target materials. Furthermore, material parameters $\Lambda_B(Z_T)$ for a large number (27) of elemental massive solid samples are available from the work of Hasselkamp *et al.* [23].

The difference in the forward and backward emission is due to energy transport by recoiling electrons away from the region near the entrance surface or into the region near the exit surface. This can be specified quantitatively by the dimensionless factors

$$1-\beta_F=\beta_B=\beta . \tag{7}$$

The value of β can be obtained by measuring the Meckbach factor, i.e., forward- to backward-electron yield ratio R for fast protons,

$$R=\gamma_F/\gamma_B=\beta_F/\beta_B=(1-\beta)/\beta . \tag{8}$$

It is of common interest to use universal material parameters

$$\Lambda(Z_P,q_i,v_P,\cdots)=\mathrm{const}=f(Z_T) \tag{9}$$

not only for proton impact, but also for *heavy-ion* impact. Therefore, it is convenient to extend the yield equations (4) of the transport theory by introducing projectile-dependent (Z_P) and charge-state-dependent (q_i) factors C_F and C_B [2] to

$$\begin{aligned}\gamma_F&=\Lambda(Z_T)(1-\beta)C_F(Z_P)S_e ,\\ \gamma_B&=\Lambda(Z_T)\beta C_B(Z_P,q_i)S_e .\end{aligned} \tag{10}$$

The factors

$$\begin{aligned}C_B&=\Lambda_B^*(Z_P,q_i)/\Lambda_B^*(Z_P=1)=S_B^*(Z_P,q_i)/S_{\mathrm{ZBL}}(Z_P) ,\\ C_F&=\Lambda_F^*(Z_P)/\Lambda_F^*(Z_P=1)=S_F^*(Z_P)/S_{\mathrm{ZBL}}(Z_P)\end{aligned} \tag{11}$$

describe the deviation of the nonequilibrium near-surface stopping power S^* from the tabulated bulk energy-loss values S_{ZBL}

$$\begin{aligned}S_B^*&=C_B S_{\mathrm{ZBL}} ,\\ S_F^*&=C_F S_{\mathrm{ZBL}} ,\end{aligned} \tag{12}$$

which can be caused by several physical mechanisms such as, e.g., charge exchange, screening effects, projectile excitation or projectile ionization, or even molecular-

orbital excitation [2,10]. It should be noted that strong *forward* effects concerning the dependence of electron yields on the charge state q_i of the ions can only be expected if the thickness d of the foil is smaller than (or comparable to) the charge-equilibration depth λ_{eq} and the *range of fast electrons* from binary collisions or from projectile ionization. In the following, we will discuss results obtained with foils thick enough to ensure charge equilibration.

From Eqs. (10)–(12) we see that the Meckbach factor for heavy-ion impact is given by

$$R=\gamma_F/\gamma_B=\frac{(1-\beta)}{\beta}S_F^*/S_B^* \ . \tag{13}$$

If the effective stopping power near the entrance surface, S_B^*, is approximately equal to the effective stopping power near the exit surface, S_F^*, Eq. (8) is also valid for heavy-ion impact, see below, Eq. (16).

III. EXPERIMENT: PROJECTILE- AND CHARGE-STATE DEPENDENCE OF ELECTRON YIELDS

In the following, we present a summary of results on the projectile (Z_P) dependence and charge-state (q_i) dependence of ion-induced electron emission. All the data have been obtained with "thin" foil targets thick enough to allow charge equilibration of the ions.

Recently, Clouvas *et al.* published values for the parameters $\Lambda_T^*(Z_P,Z_T=6)$ obtained with different ions ($Z_P=1,3,6,7,8,9,13,16,17,26$) [10] from measurements of the total electron yield γ_T from carbon foils in a standard high vacuum (HV) of 10^{-6} Torr. The factors

$$C_T(Z_P)=\Lambda_T^*(Z_P)/\Lambda=\Lambda_T^*(Z_P)/\Lambda_T^*(Z_P=1) \tag{14}$$

with $C(Z_P=1)=1$ are shown in Fig. 1 as a function of the projectile atomic number Z_P (open circles). Also shown are C_T values obtained from singly-charged-ion bombardment ($Z_P=1,2,6,8,10$) of sputter-cleaned carbon foils in ultrahigh vacuum (UHV) of 10^{-9} Torr taken from Refs. [2] and [17]. The UHV results of Refs. [2] and [17] were obtained with the same experimental setup. Note: from Eqs. (2) and (11) it follows that $C_T \neq C_B + C_F$.

Both data sets show a decrease of C_T with Z_P. The HV data reach an equilibrium value of $C_T^{HV}(Z_P \geq 6)=0.57$ for $Z_P \geq 6$ corresponding to a value of $\Lambda_T^*=(0.4\pm0.1)$ Å/eV [10]. It is worth noting that the value of the parameter $C_T(Z_P=6)=0.61$ calculated from results published by Kroneberger *et al.* [5] and Koschar *et al.* [6], which were obtained with an identical experimental setup in HV, is in good agreement with the recent results of Clouvas *et al.* [10]. Also, the UHV data suggest that the $C_T(Z_P)$ values converge against a value of $C_T^{UHV}(Z_P \gg 6)\approx 0.4$.

Probably, the difference in the absolute value of $C_T^{HV}(Z_P \geq 6)$ and $C_T^{HUV}(Z_P \gg 6)$ can be explained by the strong dependence of electron emission on surface contamination and structure. The electron yield from a sputter-cleaned surface in ultrahigh vacuum is lower than the yield from a contaminated, untreated surface. The sputtering process both cleans and smooths the surfaces

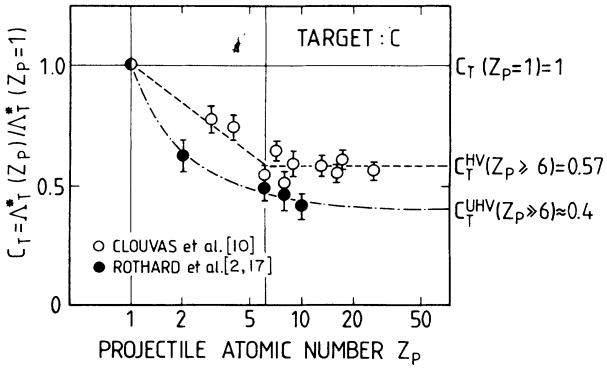

FIG. 1. The parameters $C_T(Z_P)=\Lambda_T^*(Z_P)/\Lambda=\Lambda_T^*(Z_P)/\Lambda_T^*(Z_P=1)$ obtained with different ions ($Z_P=1,3,6,7,8,9,13,16,17,26$) from measurements of the total electron yield γ_T from carbon foils in a standard high vacuum (HV) of 10^{-6} Torr [10] (open circles) as a function of the projectile atomic number Z_P [normalized to $C(Z_P=1)=1$]. Also shown are C_T values obtained from singly-charged-ion bombardment ($Z_P=1,2,6,8,10$) of sputter-cleaned carbon foils in ultrahigh vacuum (UHV) of 10^{-9} Torr taken from Refs. [2] and [17].

by preferential sputtering. The following arguments explain the electron-yield reduction for a cleaned surface: A layer of adsorbates on a clean metal surface can lead to a reduction of the electron work function Φ [1,20] causing an enhanced surface-transmission probability. Layers of oxides or insulating adsorbates lead to a larger electron-escape depth λ and thus to a higher yield. Also, the change of the composition (i.e., the target material Z_T) of the near-surface layers affects the stopping power S_e and thus the production of electrons. Furthermore, it can be shown that a rough, uncleaned surface is associated with an enhanced electron-escape probability compared to a smooth, planar surface. More details on the dependence of electron emission on surface properties can be found in Refs. [1,9,19,20].

Recently, a pronounced increase of $R(Z_P)$ with Z_P from sputter-cleaned foil surfaces was reported [2]. Figure 2 presents the data taken from Ref. [2] enriched with

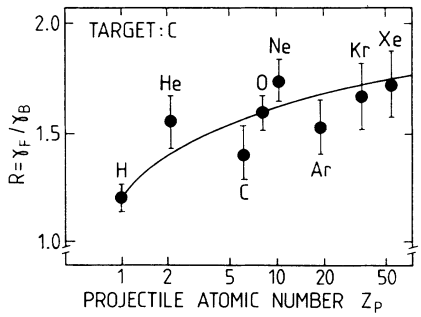

FIG. 2. The Meckbach factors $R(Z_P)=\gamma_F/\gamma_B$ [2,17] for $Z_P=1,2,6,8,10,18,36,54$ ($q_i=1$) and carbon targets. It is important to note that the results for $R(Z_P)$ shown in Fig. 2 have not been obtained for the same projectile velocity, but for the same absolute projectile energy of $E_P \approx 1.2$ MeV for $Z_P < 10$ and $E_P \approx 2.4$ MeV for $Z_P \geq 10$.

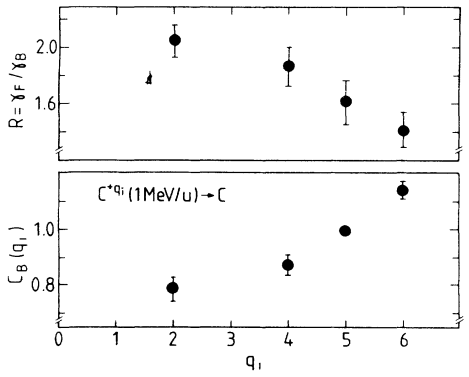

FIG. 3. The parameter $C_B(q_i)=\Lambda_B(q_i)/\Lambda_B(q_i\approx q_f)=\gamma_B(q_i)/\gamma_B(q_i\approx q_f)$ as a function of the charge state q_i of C^{q_i+} ions (1 MeV/u) [5,6] (bottom). Also shown are the Meckbach factors $R(q_i)=\gamma_F/\gamma_B(q_i)$ (top).

further data from Ref. [17] for carbon targets and $Z_P=1,2,6,8,10,18,36,54$ ($q_i=1$). R is clearly increasing with increasing projectile atomic number Z_P (see Sec. IV A). It is important to note that the results for $R(Z_P)$ shown in Fig. 2 have not been obtained for the same projectile velocity, but for the same absolute projectile energy of $E_P\approx 1.2$ MeV for $Z_P<10$ and $E_P\approx 2.4$ MeV for $Z_P\geq 10$. The dependence of backward-electron yields on the charge state of the incoming ions is demonstrated by Fig. 3. This figure shows the parameter

$$C_B(q_i)=\Lambda_B(q_i)/\Lambda_B(q_i\approx q_f)=\gamma_B(q_i)/\gamma_B(q_i\approx q_f) \quad (15)$$

as a function of the charge state q_i of C^{q_i+} ions (1 MeV/u) [5,6]. Since we expect the effective stopping power of the ions to be approximately equal at both the entrance and the exit surfaces if the charge state q_i of the incoming ions is equal to the final charge q_f, we define

$$q_i=q_f(\approx q_{\text{eff}})\leftrightarrow S_F^*\approx S_B^*\rightarrow \begin{cases} C_B(q_i\approx q_f)=1 \\ R(q_i\approx q_f)=(1-\beta)/\beta \end{cases} . \quad (16)$$

In the case of C (1 MeV/u), $q_f=5.0$ [24] and thus $C_B(q_i=5)=1$. Also shown are the Meckbach factors $R(q_i)=\gamma_F/\gamma_B(q_i)$. According to (16), the value of the transport factor β can be obtained by comparing heavy-ion-induced electron yields $\gamma_B(q_i\approx q_f)$ and γ_F from Eq. (8).

IV. THE CONCEPT OF THE PREEQUILIBRIUM NEAR-SURFACE STOPPING POWER

The interaction of ions with matter leads to the liberation of electrons ("primary ionization," PI). The energy and angular distribution of these primarily liberated electrons can in principle be obtained from ion-atom collision experiments under single-collision conditions. These "primaries" may ionize further target atoms in condensed matter and thus create a cascade of secondary electrons ("cascade multiplication," CM).

The electron-yield equations can be written as a product [compare with Eq. (4)] of (1) the (effective) stopping power S_e^* which accounts for the production of primaries, (2) the "transport factor" β, and (3) the target-material-dependent parameter Λ which accounts for the cascade multiplication (depending on the low-energy electron stopping and the surface-transmission probability) only if the contribution of cascade electrons to the total yield is dominant. If this assumption is valid, the low-energy electron distribution should be similar for all charged projectiles. Indeed, the low-energy electron spectrum does not show a strong dependence on the type of projectile, i.e., it is quite similar for (fast) electron, proton, and heavy-ion impact [1,2].

Furthermore, the major part of the energy lost by the ions causes the production of electrons with energies much higher than the mean electron energy ($\approx$20–30 eV) [1,6]. It is conceivable that these electrons are likely to contribute strongly to CM. The basic property of metals is that the outer-shell electrons are nonlocalized and behave as nearly free electrons. This means that also low-energy primary or secondary electrons with energies below the mean electron energy can easily transfer energy to the conduction electrons and significantly contribute to CM. This is not the case in insulators, where a minimum energy is required for the ionizing particle to liberate the target electrons.

The extension [2] of the yield equations (4)–(8) of Schou's transport theory Eqs. (4)–(8) [22] to Eqs. (9)–(13) is based on several other assumptions on the transport factor β, the contribution of cascade multiplication, and the spectrum of primarily ionized electrons. The starting point for our analysis is the discussion of the transport factor β in Sec. IV A. The energy spectrum of primarily ejected electrons ("primary spectrum") will be discussed in Sec. IV B and the evolution of the ionic charge state in connection to the concept of the preequilibrium stopping power in Sec. IV C. In particular, the question of target- and projectile-excitation (TE and PE, respectively) processes which may contribute to a reduction of electron yields by "taking away" some of the electronic energy loss without creating electrons (which has so far been disregarded) will be addressed.

A. The transport factor β

The parameter β in Eqs. (4)–(13) accounts for energy transport by high-energy electrons, compare the discussion in Refs. [22] and [2], and was assumed to be independent of the projectile-target combination, i.e., β does not depend on the projectile nuclear charge Z_P. In particular, $\beta(Z_P)=$const means that the primary spectrum should be similar for heavy- and light-ion impact at high primary energies above the mean secondary or cascade electron energy (i.e., $E\gg$20–30 eV). Such high-energy electrons largely contribute to CM. As will be shown below (Sec. IV B), the primary spectrum scales approximately with Z_P^2 for high primary energies. Thus the energy transport away from the backward-surface or into the forward-surface region is similar for different Z_P, i.e., $\beta(Z_P)=$ const. Also, convoy-electron production and

even projectile electron loss in the forward direction represent only a very small fraction (some percent) of all charge exchange events [4] and should not lead to major differences in energy transport by fast electrons.

As we have pointed out in Sec. III, Eq. (16), measurements of $R(Z_P)$ with ions of a charged state q_i close to the final charge state q_f may possibly be used to obtain the dependence of the transport parameter β on the projectile nuclear charge. As $R(v_P)$ was found to increase with the projectile velocity for $E_P/M_P < 200$ keV/u, only R values obtained with ions of sufficiently high velocities ($E_P/M_P > 150$ keV/u) have to be taken into account. In Table I we present a compilation of the available experimental results on the dependence of R on Z_P. We have included results which approximately satisfy the condition Eq. (16), i.e., $q_i \approx q_f$, by arbitrarily including data with $|q_i - q_f| \leq 1$ or $0.65 < q_i/q_f < 1.4$ only.

The results belong to four different classes: (1) carbon targets, high vacuum, (2) carbon targets, ultrahigh vacuum, (3) aluminum targets, and (4) gold targets. The results of classes (1) and (2) yield values of $0.39 \leq \beta \leq 0.46$ for $Z_P = 1$, $\beta \approx 0.39$ for $Z_P = 2$, and $0.32 \leq \beta \leq 0.38$ for $5 \leq Z_P \leq 8$. Thus these results suggest a weak dependence of β on Z_P, i.e., $\beta \approx 0.35$ for $Z_P > 2$, $\beta \approx 0.39$ for $Z_P = 2$, and $\beta \approx 0.43$ for $Z_P = 1$. In contrast, the results obtained by Koyama *et al.* [12] with gold targets (4) at high projectile velocities (≈ 6.2 MeV/u) with bare incident ions ($2 \leq Z_P \leq 8$) do not show a Z_P dependence, i.e., $\beta(Z_P) = \text{const} \approx 0.4$. The data from (oxidized) aluminum (3) for $Z_P = 1,2$ scatter around a value of $\beta \approx 0.43$.

In conclusion, the value of the transport factor β may slightly depend on the projectile atomic number Z_P, however, we find a mean value of $\beta \approx 0.40 \pm 0.06$. Thus the possible Z_P-dependent deviation of $\beta(Z_P)$ from this value is less than 15%. This finding is strongly supported by theoretical calculations within the transport theory. Such calculations show that β can be expected to be constant within $\pm 15\%$ for different projectile-target combinations [22] at sufficiently high velocities ($E_P/M_P > 150$ keV/u).

B. The energy spectrum of primarily ejected electrons

Although energy and angular distributions of electrons from light-ion collisions with atoms, i.e., with gas targets under single-collision conditions, have been studied extensively both experimentally and theoretically, little was known about the projectile dependence of electron spectra from heavier-ion impact. In a recent review, Toburen [25] presented angle-integrated electron spectra $d\sigma(E_e)/dE_e$ for H^+, He^+, and C^+ collisions with Ar (10 eV $\leq E_e \leq$ 1000 eV). These spectra, shown in Fig. 4, were taken at the same ion velocity for the three ions ($v_P = 3.46 v_B$, corresponding to $E_P/M_P = 300$ keV/u, $v_B = v_0$ denotes the Bohr velocity). The cross sections have been divided by the square of the projectile nuclear charge, Z_P^2. Scaled in this way, "*. . . the cross sections for ejection of the high-energy electrons are in surprisingly good agreement*" [25].

At high energies, i.e., for electrons resulting from collisions with small impact parameter ($E > 200$ eV), the primary spectrum is quite similar, and the absolute magni-

TABLE I. Compilation of the available experimental results on the dependence of R on Z_P. Also shown are the charge states q_i of the incoming ions and the mean charge q_f as calculated from Shima, Ishihara, and Mikumo [24]. We have included results which approximately satisfy the condition Eq. (6), i.e., $|q_i - q_f| \leq 1$ or $0.65 < q_i/q_f < 1.4$ only. As $R(v_P)$ was found to increase with the projectile velocity for $E_P/M_P < 200$ keV/u, only R values obtained with ions of sufficiently high velocities ($E_P/M_P > 150$ keV/u) have been included. Also shown are the values of transport parameters β calculated from Eq. (13) (see text).

Z_P	Z_T	E_P/M_P	q_i (MeV/u)	q_f	R	β	Reference	Remarks
1	6	1.2	1	1.0	1.15	0.46	Kroneberger *et al.* [5]	HV
5	6	0.3	3	3.25	2.16	0.32	Dednam *et al.* [15]	HV
6	6	1.0	5	5.0	1.63	0.38	Koschar *et al.* [6]	HV
8	6	0.26	3	4.47	2.00	0.33	Shi *et al.* [13]	HV
8	6	0.2	4	4.27	2.11	0.32	Dednam *et al.* [15]	HV
8	6	0.2	5	4.27	2.05	0.33	Dednam *et al.* [15]	HV
1	6	0.25	1	0.87	1.55	0.39	Meckbach, Braunstein, and Arista [11]	UHV
1	6	1.2	1	1.0	1.2	0.45	Rothard *et al.* [17]	UHV
2	6	0.6	1	1.81	1.55	0.39	Rothard *et al.* [17]	UHV
1	13	2.0	1	1.0	1.4	0.42	da Silveira and Jeronymo [16]	HV, Al_2O_3
2	13	0.25	1	1.73	1.8	0.36	da Silveira and Jeronymo [16]	HV, Al_2O_3
2	13	0.5	1	1.73	1.3	0.44	da Silveira and Jeronymo [16]	HV, Al_2O_3
2	13	0.5	1	1.73	1.3	0.44	da Silveira and Jeronymo [16]	HV, Al_2O_3
1	13	1.2	1	1.0	1.1	0.48	Rothard *et al.* [17]	UHV
2	79	6.2	2	1.99	1.37	0.42	Koyama *et al.* [12]	10^{-8} Torr
7	79	6.2	7	6.52	1.54	0.39	Koyama *et al.* [12]	10^{-8} Torr
8	79	6.2	8	7.43	1.49	0.40	Koyama *et al.* [12]	10^{-8} Torr

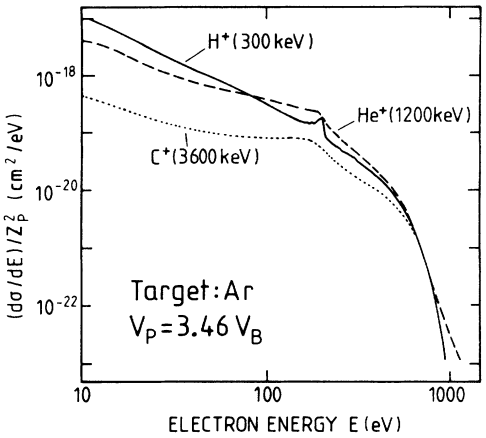

FIG. 4. Angle-integrated electron spectra $d\sigma(E_e)/dE_e$ for H^+, He^+, and C^+ collisions with Ar ($10 \le E \le 1000$ eV) taken from the review article of Toburen [25]. The spectra were taken at the same ion velocity for three ions ($v_P = 3.46 v_B$, corresponding to $E_P/M_P = 300$ keV/u). The cross sections have been divided by the square of the projectile nuclear charge, Z_P^2.

tude scales as the energy loss of bare, high-velocity ions would, i.e., with Z_P^2. At low electron energies and thus larger impact parameters, the Z_P^2 scaled spectra differ significantly and the cross sections depend on the projectile, i.e.,

$$\frac{d\sigma(H^+)/dE}{1} > \frac{d\sigma(He^+)/dE}{4} > \frac{d\sigma(C^+)/dE}{36} . \quad (17)$$

This can be explained by a screening of the projectile charge by the projectile electrons, a mechanism closely related to the effective-charge concept.

The above-quoted electron-emission cross sections are given in absolute units and can thus be used to calculate the fraction of the stopping power which has been transferred to "secondary" electrons (S_{SE}) by

$$S_{SE} = \int_{E_i}^{E_f} T \frac{d\sigma(E)}{dE} dE \quad (18)$$

with $T = E + V$, $V = 15.75$ eV being the electron binding energy for Ar. $\sigma(E)$ can be well approximated by an ansatz $d\sigma(E)/dE = aE^n$ with different parameters a and n for the energy ranges $10 \le E \le 30$ eV, $30 \le E \le 200$ eV, $200 \le E \le 600$ eV, $600 \le E \le 1000$ eV. For $E < 10$ eV, the most reasonable extrapolation was to assume $d\sigma(E)/dE = \text{const} = d\sigma(10\text{ eV})/dE$ (compare also Fig. 8 of Ref. [25]). By summing up the stopping powers obtained for the different energy ranges, we can obtain (Table II) the total stopping power leading to electron creation, S_{SE}, and compare this quantity to the tabulated values S_{ZBL} [21].

The results are summarized in Table II. Surprisingly, we find $r_{TE} \approx S_{SE}/S_{ZBL} \approx 0.8$ for H^+ and He^+, but $r_{TE} \approx S_{SE}/S_{ZBL} \approx 0.5$ for C^+. Thus approximately 20% of the total energy lost leads to nonionizing excitation of the target atoms (TE) in the case of light-ion impact on a structured target. In the case of the heavier ion (C^+), even more energy is transferred to nonionizing processes. In the case of ions carrying many electrons, projectile excitation (PE) may also contribute to the deviation of S_{SE} from S_{ZBL}.

C. The evolution of the ionic charge state

In this section, we will compare the effective ion charges at both the backward (q_B^*) and the forward (q_F^*) side of the foils to the values q_{ZBL} used in the stopping-power tables of Ziegler, Biersack, and Littmark [21]. The idea is illustrated by Fig. 5, which shows the dependence of the effective ion charge $q(x)$ inside a thin solid foil of thickness d as a function of the penetration depth x according to experimental results by Zaikov *et al.* [26]. λ_{eq} denotes the charge-equilibration depth, i.e., at $x = \lambda_{eq}$, the ionic charge is in equilibrium, the effective charge is $q_{eff} = q^*(x > \lambda_{eq}) = q_{ZBL}$, and the stopping power is $S_{ZBL} \sim (q_{ZBL})^2$.

For simplicity, we restrict our discussion to carbon targets and projectile velocities of ≈ 0.2–0.3 MeV/u. Since the experimental results used in Figs. 1 and 2 have been performed in the range 60 keV/u $\le E_P/M_P \le 1.8$ MeV/u, and the mean-charge data to be used in the following have been obtained at 200 eV/u—300 keV/u, this is a compromise. Note that the mean C_B and C_F values from [2] for C, Al, Ti, Ni and Cu are close to the ones obtained with C. Also, because the effective-charge values for C and N projectiles are quite similar (and not too different from the values for Ne), we shall often compare in the following the "heavy-ion" data for either C or N to the heavy-ion (Ne) and the light-ion (H, He) data. This is further justified by the finding that $C_T(Z_P)$ is constant for $Z_P \ge 6$ by Clouvas *et al.* [10] (Fig. 1).

The effective-charge values for $q^*(x > \lambda_{eq}) = q_{ZBL}$ values have been calculated according to Ref. [21]. The forward effective-charge values q_F^* have been calculated from charge-state distributions [26,27] under the assumption that the effective charge q_F^* determining the stopping

TABLE II. The fraction of the stopping power which has been transferred to "secondary" electrons, S_{SE} (calculated from Fig. 4, see text) in comparison to the tabulated stopping-power values S_{ZBL} [21], with $r_{TE} = S_{SE}/S_{ZBL}$.

Proj.	S_{SE} [eV/(10^{15} atoms/cm^2)]	S_{ZBL} [eV/(10^{15} atoms/cm^2)]	$r_{TE} = S_{SE}/S_{ZBL}$
H^+	15.7	19.6	0.80
He^+	54.8	70.3	0.78
C^+	141	291	0.49

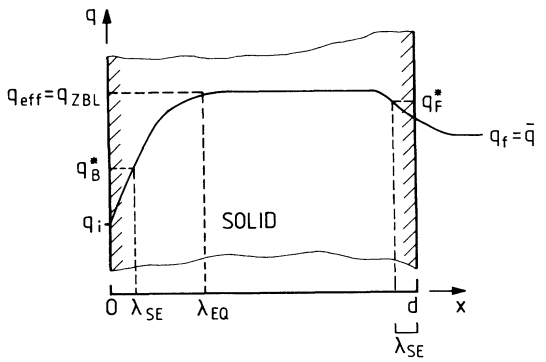

FIG. 5. The evolution of the effective ion charge $q(x)$ inside a thin solid foil of thickness d as a function of the penetration depth x according to experimental results by Zaikov *et al.* [26]. λ_{eq} denotes the charge-equilibration depth, i.e., at $x=\lambda_{eq}$, the ionic charge is in equilibrium, its effective charge is $q_{eff}=q(x>\lambda_{eq})=q_{ZBL}$, and the stopping power is $S_{ZBL}\sim(q_{ZBL})^2$.

power at the forward surface is not very different from the mean charge $\bar{q}=q_f$ of the ions. The backward effective charges q_B^* were calculated by assuming that the escape depth of low-energy SE is about $\lambda\approx 15$ Å [1,6]. From the target-thickness dependence of the mean charge $\bar{q}$ of N^{2+} ions [26] one can—as a first approach—assume that $q_B^*=\bar{q}(d=15$ Å). However, because the initial charge state of the N ions was $q_i=+2$ and the charge state of the ions used in the experiments under investigation was $q_i=+1$, this procedure may lead to an overestimation of q_B^* and thus to an underestimation of possible deviations of S^* to S_{ZBL}. In the case of H^+ and He^+, the charge-state fractions have reached an equilibrium around $d\approx 50$ Å. To obtain a first approximation for q_B^*, a linear approximation of $\bar{q}(d)$ seemed to be reasonable.

The energy-loss ratios $r_B=S_B^*/S_{ZBL}$ and $r_F=S_F^*/S_{ZBL}$, i.e., the ratios of the squares of the effective near-surface charges q_F^* and q_B^* to the squares of q_{ZBL} are shown in Table III. The quantities r_B(TE) and r_F(TE) are a direct measure of the deviation of the near-surface energy loss S^* to the calculated ZBL energy loss S_{ZBL}. A comparison to the C_F and C_B values from Fig. 1 shows that the tendency of the Z_P dependence of the C values as well as their absolute magnitude are represented within ±40%.

By taking into account that a fraction of the ion energy loss may lead to either target (or projectile) excitation, the Z_P dependence of the C factors can be estimated even more accurately: We introduce the estimates r_{TE} obtained in Sec. IV C by multiplying the "effective-charge factors" r_B and r_F with the "nonionizing target-excitation factor" r_{TE} from Table II. Furthermore, we assume that only a small fraction ($<10\%$) of the projectiles are in an excited state when leaving the foil. According to the results of Zaikov *et al.* [26] this assumption is justified and thus electron emission from excited projectiles which decay via electron emission outside the foil can be neglected. The final result for $r_{TE}r_F$ (compare to C_F) and $r_{TE}r_B$ (compare to C_B) are shown in Table III (normalized to 1 for H). The Z_P dependence of the factors C_F and C_B can be described within an error of less than 30%, a surprisingly good result.

Thus the electron yields are a function of the effective ion charges q^* very close to the surface within a depth comparable to low-energy electron-escape depths λ_{SE},

$$\gamma\sim S_{F,B}^*(x=\lambda_{SE})=C_{F,B}S_{ZBL}\sim[q_{F,B}^*(x=\lambda_{SE})]^2 . \quad (19)$$

As we have shown above, this concept of an *effective near-surface stopping power* can be used to describe the electron-yield dependence on the projectile atomic number Z_P. It can also be applied to describe the charge-state dependence of electron yields as demonstrated in Fig. 3 [1,6,28]. Recent calculations of the dependence of the energy loss of ions on the charge state of the ions inside the solid performed by Arnau *et al.* [29] strongly support this approach. A similar concept has been successfully applied to electron emission by slow ($E_P<16$ keV) H^-, H^0, and H^+ projectiles [30]. Furthermore, it has been shown that the electronic energy loss depends on both target thickness and the charge state of the ions at $v_P\gg v_B$ [31]. It has often been proposed to perform simultaneous measurements of γ and S_e. The discussion above shows, however, that only simultaneous measurements of γ and S^* may be meaningful.

TABLE III. The energy-loss ratios $r_B=S_B^*/S_{ZBL}$ and $r_F=S_F^*/S_{ZBL}$, i.e., the ratios of the squares of the effective near-surface charges q_F^* and q_B^* to the squares of q_{ZBL} and the "effective-charge factors" r_B and r_F multiplied with the "nonionizing target-excitation factor" r_{TE} from Table II (see text) in comparison to the factors C_F and C_B (from Refs. [2] and [17]) for different ions ($Z_P=1,2,6,7,8,10$).

Proj.	Z_P	C_B	r_B	r_Br_{TE}	C_F	r_F	r_Fr_{TE}
H	1	**1.00**	1.00	**1.00**	**1.00**	1.00	**1.00**
He	2	**0.60**	0.45	**0.44**	**0.65**	0.82	**0.80**
C	6	**0.40**			**0.60**		
O	8	**0.36**			**0.58**		
N	7		0.47	**0.30**		0.67	**0.42**
Ne	10	**0.32**			**0.49**		

The C factors describe the deviation of the near-surface stopping power (connected to electron emission) to the tabulated values, see Eqs. (11), (12), and (19). The possible behavior of these factors taking into account Figs. 1 and 5 and Table III is summarized in Table IV. In the case of (fast, i.e., $q_f \approx 1$) hydrogenic projectiles, C_F and C_B are (per definition) equal to one (C_B: proton impact only) if the target is thick enough to allow charge equilibration. In the case of H^0 or H^- impact, C_B may be larger than one at high velocities because the projectile electrons can contribute to additional electron emission [1,5,18] either via kinetic secondary electron emission [5,18] or as loss electrons [32]. At low velocities ($v_P < 2-3v_B$), however, C_B may be smaller than one because screening of the projectile nuclear charge occurs if the velocity of the projectile electrons is comparable to or lower than the projectile velocity [1,5,18,30].

For heavier particles ($Z_P \geq 2$), C_B is lower than one if the charge state q_i of the incoming ions is lower than the mean charge q_f, and larger than one if $q_i > q_f$. This is most clearly demonstrated in Fig. 3, but leads also to the Z_P dependence shown in Fig. 1 and, in particular, to the Z_P dependence of the Meckbach factor R shown in Fig. 2 (compare the discussion in Ref. [2]). As long as the low-energy electron-escape depth λ_{SE} is lower than the charge equilibration depth λ_{eq}, $\lambda_{SE} \ll \lambda_{eq}$, i.e., at high enough velocities, C_B can be expected to depend only weakly on the projectile velocity. It is this situation which is sketched in Fig. 5. Even for the impact of bare ions of very high velocities $E_P/M_P > 5$ MeV/u with $q_b = q_{eff} = q_f$ on solids, a reduction $C_B < 1$ has been reported [33].

If $q_i < q_{ZBL}$ or $q_f < q_{ZBL}$, the dependence of $C \sim q^{*2}$ on Z_P results in a *depression* of electron yields with increasing Z_P. Interestingly, such a suppression of low-energy electrons under heavy-ion impact can be seen both for *primary ionization* (single-collision conditions, see, e.g. [25,35], and Fig. 4) and *(cascade) electrons* from solids [36,37]. A variety of different mechanisms have been discussed in this context, but it is still unclear in what magnitude each of them contributes to the low-energy electron suppression: The most important mechanisms are probably the *screening of the projectile nuclear charge by projectile electrons* [25,35] (even projectile shell effects have been observed, compare [5,6]) and the *screening of the projectile charge by target electrons* in metals [37]. Also, changes of the surface barrier height caused by a *charging up near the ion track* [12,28], an *interaction of the ion's wake with the surface potential* [1,18], or a *depression of the SE excitation probability due to a high density of electron-hole pairs* (which then no longer remain uncorrelated) have been mentioned [37], compare Ref. [2] for a more detailed discussion.

TABLE IV. The possible behavior of the C factors describing the deviation of the near-surface stopping power (connected to electron emission) to the tabulated values [Eqs. (11), (12), (19)] for *fast* ions of $Z_P = 1$ and $Z_P \geq 2$, respectively, if the target is thick enough to allow charge equilibration (see text).

	$C_B(q_i < q_f)$	$C_B(q_i \geq q_f)$	$C_F(q_f = q^*)$
$Z_P = 1$	> 1	$= 1$	$= 1$
$Z_P > 1$	< 1	≥ 1	≤ 1

If the mean equilibrium charge of the ions outside the solid q_f was larger than the mean effective charge q_{eff} inside (Betz-Grodzins model [34]), electrons from the decay of excited projectiles should lead to additional electron emission at the exit side and thus possibly to enhanced values $C_F > 1$. This is in contrast to the findings of Zaikov *et al.* [26] and to the results shown in Table III (compare also Fig. 5). Possibly, the capture of electrons near the target exit surface into excited states may explain these findings [26].

However, the preequilibrium evolution of the effective projectile charge q^* near the entrance surface is the key for an understanding of the dependence of the near-surface stopping power $S_B^* = C_B(Z_P)S_{ZBL}$ on the projectile atomic number Z_P and on the charge state of the ions q_i. Even at the exit surface, where a *sudden change of the projectile screening, deexcitation* of the projectile having been excited inside the solid or *capture of electrons from the target* can take place, an effective stopping power $S_F^* = C_F(Z_P)S_{ZBL}$ has to be considered. Consequently, electron emission from solid surfaces as a function of the projectile atomic number Z_P and on the charge state of the ions q_i is related to the effective stopping power S_F^* and S_B^*.

V. CONCLUSION

We have shown that the concept of the preequilibrium near-surface stopping power $S^* = C(Z_P, q_i)S_{ZBL}$ can successfully be applied to describe the dependence of ion-induced electron yields $\gamma \sim \beta S^*$ on the projectile atomic number Z_P and on the charge state q_i of the incoming ions. After having presented a summary of recent results on the projectile- and charge-state dependence of forward- and backward-electron yields γ_F and γ_B and the Meckbach factor $R = \gamma_F/\gamma_B$ we discuss the implementation of this concept into Schou's transport theory. For this aim, we propose a simple extension of the yield equations and discuss several necessary assumptions, in particular concerning the transport factor β.

By using the energy spectrum of primarily ejected electrons to estimate the energy-loss fraction leading to electron emission and, in particular, by estimating the effective charges of ions from charge-state distributions, we can even describe the Z_P dependence of the factors C_F and C_B quantitatively within an error of less than 30%. This result strongly supports the near-surface nonequilibrium stopping-power concept and thus the conclusions of Koschar *et al.* [6], Rothard *et al.* [2], and Clouvas *et al.* [10]. However, further investigations are necessary to clarify which mechanisms contribute and in what magnitude to the deviation of the near-surface stopping powers to the tabulated charge-equilibrium stopping-power values.

If this proportionality of electron yields and the stopping power can be further confirmed, electron emission may become a powerful tool to measure the energy loss of charged particles and to test energy-loss models [1,2,38].

In particular, the energy loss of molecules or clusters [5,18,38] or the dependence of the energy loss on the preequilibrium evolution of the charge state of the ions [6] can be investigated. With sufficiently thin targets or at sufficiently high ion velocities (which are accessible with heavy-ion accelerators such as GANIL at Caen, France or GSI-SIS) we are generally dealing with preequilibrium conditions where stopping-power values can significantly differ from equilibrium data and are neither available in the literature nor easily accessible experimentally.

Furthermore, ion-induced electron emission can serve as a valuable test for theories [22], which can also be applied to such fields as scanning electron microscopy and all kinds of surface analysis with Auger, photo-, or secondary electrons [19,20].

ACKNOWLEDGMENTS

It is a pleasure for us to thank Peter Koschar and Kurt Kroneberger for helpful discussions. One of us (H.R.) acknowledges the hospitality he enjoyed during his stay in Roskilde and also financial support by Risø.

*Present address: Institut de Physique Nucléaire de Lyon, Groupe des Collisions Atomiques, Université Claude Bernard, 43, Bd du 11 Novembre 1918, F-69622 Villeurbanne CEDEX, France

[1] For recent extensive reviews of charged particle induced electron emission from solids see D. Hasselkamp, H. Rothard, K. O. Groeneveld, J. Kemmler, P. Varga, and H. Winter, in *Particle Induced Electron Emission II,* edited by G. Höhler, E. A. Niekisch, and J. Treusch, Springer Tracts in Modern Physics Vol. 123 (Springer, Heidelberg, 1991). Theoretical aspects of the phenomenon are thoroughly discussed in J. Devooght, J. C. Dehaes, A. Dubus, M. Cailler, J. P. Ganachaud, M. Rössler, and W. Brauer, in *Particle Induced Electron Emission I,* edited by G. Höhler, E. A. Niekisch, and J. Treusch, Springer Tracts in Modern Physics Vol. 122 (Springer, Heidelberg, 1991). For other recent reviews of ion-induced electron emission from solid surfaces see, e.g., W. O. Hofer, in *Fundamental Beam Interactions with Solids for Microscopy, Microanalysis and Microlithography,* Proceedings of the 8th Pfefferkorn Conference, May 7–12, 1989, Park City, Utah, USA, edited by J. Schou, P. Kruit, and D. E. Newbury [Scanning Microsc. Suppl. **4**, 265 (1990)]; B. A. Brusilovsky, Appl. Phys. A **50**, 111 (1990); D. Hasselkamp, Habilitationsschrift, Justus-Liebig-Universität, Giessen, Germany, 1985; and Comments At. Mol. Phys. **21**, 241 (1988).

[2] H. Rothard, K. Kroneberger, A. Clouvas, E. Veje, P. Lorenzen, N. Keller, J. Kemmler, W. Meckbach, K.-O. Groeneveld, Phys. Rev. A **41**, 2521 (1990). See also H. Rothard, K. O. Groeneveld, and J. Kemmler, in *Particle Induced Electron Emission II* (Ref. [1]).

[3] T. Brohm, H.-G. Clerc, B. Voss, C. Ziegler, H. Geissel, M. Kildir, K.-H. Schmidt, K. Sümmerer, and D.-J. Viera, Verh. Dtsch. Phys. Ges. **26**, 414 (1991); A. Albert, K. Kroneberger, O. Heil, H. Geissel, and K. O. Groeneveld, *ibid.* **26**, 707 (1991).

[4] *Forward Electron Emission in Ion Collisions,* edited by K. O. Groeneveld, W. Meckbach, and I. A. Sellin, Lecture Notes in Physics (Springer-Verlag, Heidelberg, 1984); K. O. Groeneveld, Nucl. Tracks Radiat. Meas. **15**, 51 (1988); Radiat. Eff. Defects Solids **110**, 121 (1989).

[5] K. Kroneberger, A. Clouvas, G. Schlüssler, P. Koschar, J. Kemmler, H. Rothard, C. Biedermann, O. Heil, M. Burkhard, and K. O. Groeneveld, Nucl. Instrum. Methods B **29**, 621 (1988); K. Kroneberger, H. Rothard, M. Burkhard, J. Kemmler, P. Koschar, O. Heil, C. Biedermann, S. Lencinas, N. Keller, P. Lorenzen, D. Hofmann, A. Clouvas, E. Veje, and K. O. Groeneveld, J. Phys. (Paris) Colloq. **50**, C2-99 (1989).

[6] P. Koschar, K. Kroneberger, A. Clouvas, M. Burkhard, W. Meckbach, O. Heil, J. Kemmler, H. Rothard, K. O. Groeneveld, R. Schramm, and H.-D. Betz, Phys. Rev. A **40**, 3632 (1989).

[7] G. Schneider, Ann. Phys. (Leipzig) **5**, 357 (1931).

[8] See, e.g., H. G. Clerc, H. J. Gerhardt, L. Richter, and K. H. Schmidt, Nucl. Instrum. Methods **113**, 325 (1973); J. Schader, B. Kolb, K. D. Sevier, and K. O. Groeneveld, *ibid.* **151**, 563 (1978); H. P. Garnir, P. D. Dumont, and Y. Baudinet-Robinet, *ibid.* **202**, 187 (1982); H. J. Frischkorn and K. O. Groeneveld, Phys. Scr. **T6**, 89 (1983).

[9] A. Clouvas, H. Rothard, M. Burkhard, K. Kroneberger, R. Kirsch, P. Misealidis, A. Katsanos, C. Biedermann, J. Kemmler, and K. O. Groeneveld, Phys. Rev. B **39**, 6316 (1989).

[10] A. Clouvas, A. Katsanos, B. Farizon-Mazuy, M. Farizon, and M. J. Gaillard, Phys. Rev. B **43**, 2498 (1991).

[11] W. Meckbach, G. Braunstein, and N. Arista, J. Phys. B **8**, L344 (1975).

[12] A. Koyama, T. Shikata, H. Sakairi, and E. Yagi, Jpn. J. Appl. Phys. **21**, 1216 (1982).

[13] C. R. Shi, H. S. Toh, D. Lo, R. P. Livi, M. H. Mendenhall, D. Z. Zhang, and T. A. Tombrello, Nucl. Instrum. Methods B **9**, 263 (1985).

[14] J. C. Dehaes, J. Carmeliet, and A. Dubus, Nucl. Instrum. Methods B **13**, 627 (1986).

[15] C. C. Dednam, S. Froneman, D. W. Mingay, and J. Van Waart, Nucl. Instrum. Methods B **24/25**, 366 (1987).

[16] E. F. da Silveira and J. M. F. Jeronymo, Nucl. Instrum. Methods B **24/25**, 534 (1987).

[17] H. Rothard, K. Kroneberger, M. Burkhard, J. Kemmler, P. Koschar, O. Heil, C. Biedermann, S. Lencinas, N. Keller, P. Lorenzen, D. Hofmann, A. Clouvas, K. O. Groeneveld, and E. Veje, Radiat. Eff. Defects Solids **109**, 281 (1989).

[18] H. Rothard, K. Kroneberger, E. Veje, J. Kemmler, P. Koschar, O. Heil, S. Lencinas, N. Keller, P. Lorenzen, D. Hofmann, A. Clouvas, and K.-O. Groeneveld, Phys. Rev. B **41**, 3959 (1990).

[19] M. Burkhard, H. Rothard, J. Kemmler, K. Kroneberger, and K. O. Groeneveld, J. Phys. D **21**, 472 (1988); P. Lorenzen, H. Rothard, K. Kroneberger, J. Kemmler, M. Burkhard, and K. O. Groeneveld, Nucl. Instrum. Methods A **282**, 213 (1989); H. Rothard, M. Schosnig, K. Kroneberger, and K. O. Groeneveld, in *Interaction of Charged Particles with Solids and Surfaces,* edited by F. Flores, H. M. Urbassek, N. Arista, and A. Gras-Marti (Plenum, New York, 1991); M. Schosnig, H. Rothard, K. Kroneberger, D. Schlössler, and K. O. Groeneveld, Nucl. Instrum.

Methods B (to be published).

[20] E. Sanchez, L. F. de Ferrariis, and S. Suarez, Nucl. Instrum. Methods B **43**, 29 (1989); E. Sanchez, Nucl. Instrum. Methods A **280**, 433 (1989).

[21] J. F. Ziegler, J. P. Biersack, and U. Littmark, *The Stopping and Range of Ions in Matter* (Pergamon, New York, 1985).

[22] J. Schou, Phys. Rev. B **22**, 2141 (1980); Scanning Microsc. **2**, 607 (1988).

[23] D. Hasselkamp, S. Hippler, A. Scharmann, and T. Schmehl, Ann. Phys. (Leipzig) **47**, 7 (1990).

[24] K. Shima, T. Ishihara, and T. Mikumo, At. Data Nucl. Data Tables **34**, 357 (1986).

[25] L. Toburen, in *Fundamental Beam Interactions with Solids for Microscopy, Microanalysis and Microlithography,* Proceedings of the 8th Pfefferkorn Conference, May 7–12, 1989, Park City, Utah, USA, edited by J. Schou, P. Kruit, and D. E. Newbury [Scanning Microsc. Suppl. **4**, 239 (1990)].

[26] Z. P. Zaikov, E. A. Kralinka, V. S. Nikolaev, Yu. A. Feinberg, and N. F. Vorobief, Nucl. Instrum. Methods B **17**, 97 (1986); compare also Z. P. Zaikov, E. A. Kralinka, V. S. Nikolaev, and E. I. Sirotinin, *ibid.* **33**, 202 (1988).

[27] C. Biedermann, J. Kemmler, H. Rothard, M. Burkhard, O. Heil, P. Koschar, K. Kroneberger, and K. O. Groeneveld, Phys. Scr. **37**, 27 (1988).

[28] A. Koyama, T. Shikata, H. Sakairi, and E. Yagi, Jpn. J. Appl. Phys. **21**, 586 (1982).

[29] A. Arnau, M. Peñalba, P. M. Echenique, F. Flores, and R. H. Ritchie, Phys. Rev. Lett. **65**, 1024 (1990).

[30] G. Lakits, A. Arnau, and H. Winter, Phys. Rev. B **42**, 15 (1990).

[31] N. E. B. Cowern, P. M. Read, and C. J. Sofield, Nucl. Instrum. Methods B **12**, 43 (1985).

[32] H. Rothard, K. Kroneberger, E. Veje, M. Schosnig, P. Lorenzen, N. Keller, J. Kemmler, C. Biedermann, A. Albert, O. Heil, and K.-O. Groeneveld, Nucl. Instrum. Methods B **48**, 616 (1990).

[33] J. E. Borovsky and D. M. Suszcynsky, Phys. Rev. A **43**, 1416 (1991).

[34] H. D. Betz and L. Grodzins, Phys. Rev. Lett. **25**, 211 (1970); see also H.-D. Betz, Rev. Mod. Phys. **44**, 465 (1972).

[35] J. Schader, R. Latz, M. Burkhard, H. J. Frischkorn, D. Hofmann, P. Koschar, K. O. Groeneveld, D. Berenyi, A. Köver, and Gy. Szabo, Nuovo Cimento **7D**, 219 (1986); J. Phys. Lett. (Paris) **45**, L249 (1984).

[36] F. Folkmann, K. O. Groeneveld, R. Mann, S. Schumann, and R. Spohr, Z. Phys. A **275**, 229 (1975).

[37] A. Koyama, H. Ishakawa, Y. Sasa, O. Benka, and M. Uda, Nucl. Instrum. Methods B **33**, 338 (1988).

[38] H. Rothard, J. Schou, P. Koschar, and K. O. Groeneveld, Nucl. Instrum. Methods B (to be published).